J. Fluid Mech. (1988), *vol.* 186, *pp.* 147–162
Printed in Great Britain

Note on Bragg scattering of water waves by parallel bars on the seabed

By CHIANG C. MEI, TETSU HARA AND MAMOUN NACIRI
Department of Civil Engineering, Massachusetts Institute of Technology, Cambridge, MA 02139, USA

(Received 23 February 1986)

A recent theory of Bragg scattering of surface waves by sinusoidal sandbars on a seabed is applied to three cases not examined heretofore: (1) oblique incidence on a strip of infinitely long bars, (2) oblique incidence on the corner of a bar field and (3) seabed with a mean slope. While the Bragg mechanism has been studied previously for sandbars present on many shorelines, it can be a basis for breakwaters where the soil is not strong enough to support a single massive breakwater.

1. Introduction

It has been widely known that excessive pumping of ground water can cause subsidence of the land surface. Examples of such hazards are well recorded for Venice, Mexico City, Bangkok, etc. Despite the fact that oil is usually pumped from much greater depths, prolonged pumping over a wide area has similar effects, as is the case for the Wilmington oil field in California. Once subsidence becomes intolerable, pumping must be stopped or reduced. Recently one of the world's major offshore oil fields, the Ekofisk of the North Sea, has been plagued by this problem. Since 1979 there has been a subsidence at the rate of 45 cm per year, which of course endangers the safety of the drilling platforms against storm waves, and has prompted the Phillips Petroleum Co of Norway to seek remedies. According to MaCabe (1986), three measures have been considered: recharging the oil reservoirs with gas and water, raising the deck heights of the platforms, and constructing large breakwaters facing the prevailing waves.

Whatever decision is made for Ekofisk, it is still worthwhile to examine the various measures from the engineering viewpoint so as to be better prepared for future occurrences elsewhere. For the Ekofisk case, the breakwater option has been studied theoretically and experimentally by Norksk Hydro Inc. of Bergen, Norwave Inc. of Oslo and the Norwegian Hydrodynamics Laboratories of Trondheim. They propose a system of massive breakwaters on the windward side of the oil field. In water of 70 m depth, the concrete breakwaters would have a height of about 45–50 m, i.e. the top is submerged by the depth 20–25 m which would not interfere with navigation. Based on their studies, the potential effectiveness of such breakwaters against waves appears to be quite reasonable.

There are several circumstances under which massive breakwaters may not be the most desirable remedy. Near a coast where the water depth is small, the necessary height of a conventional breakwater would interfere with navigation. If the top soil of the seabed is weak, cyclic stresses and pore pressure induced at the footing of a large breakwater may be so great as to cause soil liquefaction and failure. Lastly, since subsidence is caused by the weight of the seabed soil itself, the additional

weight of a massive structure can induced further settlement in its vicinity. While these factors may or may not be serious enough at Ekofisk, they can be relevant in another locale. Therefore, it is worthwhile to consider alternative types of breakwater that have comparable effectiveness in protecting an area against waves, yet would cause less burden on the supporting seabed.

It is known that many naturally formed sandbars of amplitudes much smaller than the depth of the water can produce strong reflection of water waves if the bar spacing is about half of the length of normally incident waves. This mechanism is called *Bragg resonance* in crystallography and has been the subject of recent studies in water waves by a number of workers (Davis & Heathershaw 1984; Mei 1985; Kirby 1986*a*, *b*). With such a matching of phases, waves reflected from successive bars are in phase and therefore reinforce one another, resulting in strong total reflection. This means that many small structures can be as effective a breakwater as a single massive structure. Although both types of structures would require a comparable amount of material such as concrete, the weight of the parallel bars can be more evenly distributed over a much larger area of the seabed; therefore they can be more suitable than a few breakwaters on a weak seabed.

The requirement of phase matching suggests that, for a given construction of bars, the frequency and direction of the incident waves must both lie within narrow bands in order for the Bragg mechanism to be effective. It is therefore necessary to study more than just precise resonance. For parallel bars on a bed of constant mean depth, Mei (1985) and Hara & Mei (1987) have conducted both theoretical and experimental studies for normally incident waves that are slightly detuned from the resonant frequency. They have shown in particular that there exists a cutoff frequency which is proportional to the bar height. If the detuning frequency is less than the cutoff frequency, reflection increases monotonically with the increase in the number of bars. Otherwise, reflection may oscillate with the number of bars. Therefore the cutoff frequency may be regarded as the width of the frequency band within which the bars are effective as a breakwater. Under similar conditions, theoretical modifications for nonlinear effects in very shallow water have been reported by Yoon & Liu (1987).

In this note we consider three other effects which can be of interest to the dynamics of coastal processes and to the design of breakwaters: the angle of incidence, the end effects of a bar field, and the mean slope of the seabed. The theory will be based on the following asymptotic equations for the amplitudes of incident $A(x, y, t)$ and reflected wavetrains $B(x, y, t)$:

$$\frac{\partial A}{\partial t}+C_{g_1}\frac{\partial A}{\partial x}+C_{g_2}\frac{\partial A}{\partial y}+\frac{1}{2}\frac{\partial C_{g_1}A}{\partial y}=-\mathrm{i}\Omega_0\cos 2\theta B, \tag{1.1}$$

$$\frac{\partial B}{\partial t}-C_{g_1}\frac{\partial B}{\partial x}+C_{g_2}\frac{\partial B}{\partial y}-\frac{1}{2}\frac{\partial C_{g_1}B}{\partial x}=-\mathrm{i}\Omega_0\cos 2\theta A, \tag{1.2}$$

where θ is the local angle of an incident wave ray,

$$(C_{g_1}, C_{g_2}) = C_g(\cos\theta, \sin\theta) \tag{1.3}$$

are the components of the group velocity C_g in the (x, y)-directions, and

$$\Omega_0 = \frac{\omega k D}{2\sinh 2kh} \tag{1.4}$$

has the dimension of frequency. D is the amplitude of the bars, h the mean water depth, π/k the bar wavelength and ω the water-wave frequency corresponding to k

and h via the usual dispersion relation. In terms of these the incident and reflected wave potentials are

$$\Phi^{\pm} = -\frac{ig}{2\omega}\begin{pmatrix}A\\B\end{pmatrix}\frac{\cosh k(z+h)}{\cosh kh}\,e^{iS_{\pm}}, \tag{1.5a}$$

with

$$S_{\pm} = \pm\int^{x} k\cos\theta\,dx + ky\sin\theta - \omega t. \tag{1.5b}$$

The height of the parallel bars above the mean seabed is

$$\delta = \tfrac{1}{2}D\left[\exp\left(2i\int^{x} k\cos\theta\,dx\right)+\exp\left(-2i\int^{x} k\cos\theta\,dx\right)\right], \tag{1.6}$$

which satisfies the Bragg condition for resonance. Due to the mild slope of the seabed, h, k, θ, A and B are slowly varying functions of x compared with the wave phase. Detailed derivations of (1.1) and (1.2) are given in Mei (1985). These equations are valid when kA, kB, kD and $(1/kh)(dh/dx)$ are all small.

2. Oblique incidence of detuned waves on a finite strip of bars

In this section we consider parallel bars lying within the strip $0 < x < L$, with $kL \gg 1$, on a sea of constant mean depth h. The amplitudes A and B satisfy the following uncoupled equations on both sides of the strip:

$$\left.\begin{aligned}&\frac{\partial A}{\partial t}+C_{g_1}\frac{\partial A}{\partial x}+C_{g_2}\frac{\partial A}{\partial y}=0,\\&\frac{\partial B}{\partial t}-C_{g_1}\frac{\partial B}{\partial x}+C_{g_2}\frac{\partial B}{\partial y}=0,\end{aligned}\right\}\quad x<0 \quad\text{or}\quad >L. \tag{2.1}$$

Let Ω and K be the detuning frequency and wavenumber of the incident wave; then the solution must be of the form

$$\left.\begin{aligned}A &= A_0\exp[i(Kx\cos\theta+Ky\sin\theta-\Omega t)],\\B &= B_0\exp[i(-Kx\cos\theta+Ky\sin\theta-\Omega t)],\end{aligned}\right\}\quad \text{for}\quad x<0, \tag{2.2}$$

and

$$\left.\begin{aligned}A &= A_1\exp\{i[K(x-L)\cos\theta+Ky\sin\theta-\Omega t]\},\\B &= 0,\end{aligned}\right\}\quad \text{for}\quad x>L. \tag{2.3}$$

where

$$\Omega = C_g K, \quad \text{with} \quad \Omega \ll \omega, \quad K \ll k. \tag{2.4}$$

Within the strip of bars the equations are coupled:

$$\left.\begin{aligned}&\frac{\partial A}{\partial t}+C_{g_1}\frac{\partial A}{\partial x}+C_{g_2}\frac{\partial A}{\partial y}=-i\Omega_0\cos 2\theta B,\\&\frac{\partial B}{\partial t}-C_{g_1}\frac{\partial B}{\partial x}+C_{g_2}\frac{\partial B}{\partial y}=-i\Omega_0\cos 2\theta A,\end{aligned}\right\}\quad 0<x<L, \tag{2.5}$$

which can be combined to give the Klein–Gordon equation

$$\left[\left(\frac{\partial}{\partial t}+C_{g_2}\frac{\partial}{\partial y}\right)^2-C_{g_1}^2\frac{\partial^2}{\partial x^2}+(\Omega_0\cos 2\theta)^2\right]\begin{pmatrix}A\\B\end{pmatrix}=0. \tag{2.6}$$

The solution must be of the form

$$\begin{pmatrix}A\\B\end{pmatrix} = \exp[i(K\sin\theta y-\Omega t)]\left\{\begin{aligned}&A_2\,e^{ipx}+A_3\,e^{-ipx},\\&B_2\,e^{ipx}+B_3\,e^{-ipx},\end{aligned}\right\}\quad 0<x<L. \tag{2.7}$$

From the Klein–Gordon equation, we find

$$p = \frac{\Omega_0 \cos\theta}{C_g}\left[\left(\frac{\Omega}{\Omega_0}\right)^2 - \left(\frac{\cos 2\theta}{\cos^2\theta}\right)^2\right]^{\frac{1}{2}} \tag{2.8a}$$

if

$$\frac{\Omega}{\Omega_0} > \left|\frac{\cos 2\theta}{\cos^2\theta}\right| \quad \text{(above cutoff)} \tag{2.8b}$$

and

$$p = \mathrm{i}P, \quad \text{with } P = \frac{\Omega_0 \cos\theta}{C_g}\left[\left(\frac{\cos 2\theta}{\cos^2\theta}\right)^2 - \left(\frac{\Omega}{\Omega_0}\right)^2\right]^{\frac{1}{2}} \tag{2.9a}$$

if

$$\frac{\Omega}{\Omega_0} < \left|\frac{\cos 2\theta}{\cos^2\theta}\right| \quad \text{(below cutoff).} \tag{2.9b}$$

Thus

$$\Omega_0 \left|\frac{\cos 2\theta}{\cos^2\theta}\right| \tag{2.10}$$

is the cutoff frequency across which the solution changes from being monotonic to being oscillatory.

Along the edges of the bar strip, continuity of pressure and normal velocity requires that

$$\left.\begin{aligned} A_0 &= A_2 + A_3, \\ B_0 &= B_2 + B_3, \end{aligned}\right\} \quad x < 0, \tag{2.11a, b}$$

and

$$\left.\begin{aligned} A_1 &= A_2\,\mathrm{e}^{\mathrm{i}pL} + A_3\,\mathrm{e}^{-\mathrm{i}pL}, \\ 0 &= B_2\,\mathrm{e}^{\mathrm{i}pL} + B_3\,\mathrm{e}^{-\mathrm{i}pL}, \end{aligned}\right\} \quad x > L. \tag{2.12a, b}$$

Substituting (2.7) into (2.5a) and gathering the coefficients of $\mathrm{e}^{\mathrm{i}px}$ and $\mathrm{e}^{-\mathrm{i}px}$, we get two more conditions:

$$\begin{pmatrix} A_2 \\ A_3 \end{pmatrix} (\Omega \cos^2\theta \mp pC_g \cos\theta) = \Omega_0 \cos 2\theta \begin{pmatrix} B_2 \\ B_3 \end{pmatrix}. \tag{2.13}$$

We can now solve for all the coefficients A_1, A_2, A_3, B_0, B_2 and B_3 in terms of A_0. In particular the transmission T and reflection R coefficients are respectively

$$T \equiv \frac{A_1}{A_0}, \quad R \equiv \frac{\mathrm{i}B_0}{A_0}. \tag{2.14}$$

The results are given below for the *above-cutoff* case:

$$T = \frac{A_1}{A_0} = \frac{pC_g}{pC_g \cos pL - \mathrm{i}\Omega \cos\theta \sin pL} \tag{2.15}$$

and

$$R = \frac{\Omega_0 \sin pL \cos 2\theta}{\cos\theta[pC_g \cos pL - \mathrm{i}\Omega \cos\theta \sin pL]}. \tag{2.16}$$

If the detuning is below cutoff, one simply replaces p by $\mathrm{i}P$, $\sin pL$ by $\mathrm{i}\sinh PL$ and $\cos pL$ by $\cosh PL$ in the preceding formulas.

By straightforward algebra, it can be shown that

$$|R|^2 + |T|^2 = 1, \tag{2.17}$$

which is expected on the ground of energy conservation.

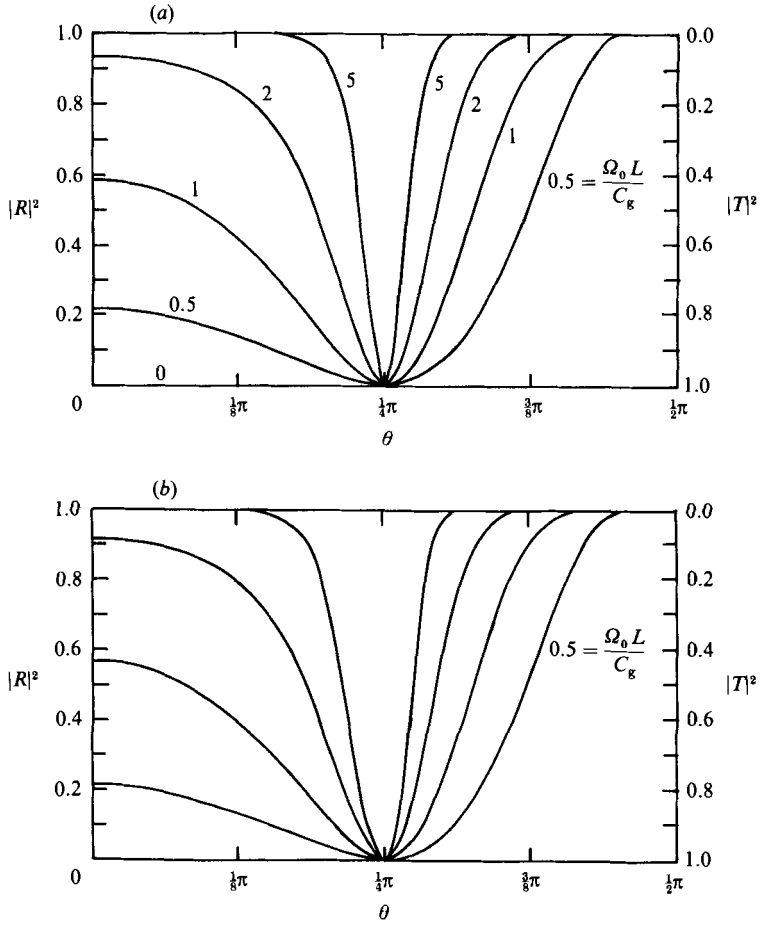

FIGURE 1 (*a*, *b*). For caption see next page.

In figure 1 we plot the magnitudes of the reflection and transmission coefficients as a function of θ with Ω/Ω_0 and $\Omega_0 L/C_g$ as parameters. Note that at the critical incidence angle $\theta = \frac{1}{4}\pi$ the bars lose all effects on waves. For small detuning Ω/Ω_0, there is only a small neighbourhood near the critical angle where reflection is small. As Ω/Ω_0 increases, this neighbourhood grows wider. The change from monotonic to oscillatory behaviour across the cutoff frequency is more clearly shown in figure 2.

3. Scattering by the corner of a bar field

In reality the bar field must be of finite horizontal extent. It would be very desirable to analyse fully the implications of Bragg resonance by parallel bars in a finite rectangle, by solving (1.1) and (1.2) with two space coordinates and time. As an alternative approach Kirby (1986*a*) has extended the mild slope equation to include the additional effects of bars and reported limited results for this problem by numerical solution. In this section we shall give the analytical solution to a simpler problem: scattering by parallel bars occupying the entire first quadrant of the (x, y)-plane, as sketched in figure 3. For mathematical expediency we shall only consider

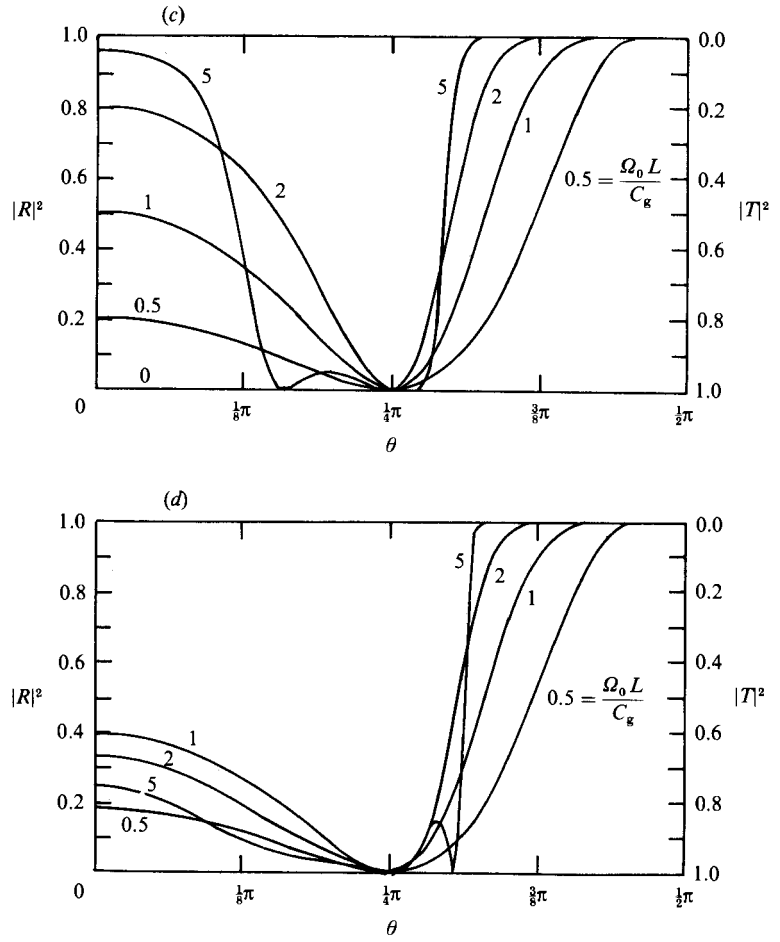

FIGURE 1. Reflection and transmission intensities $|R|^2$ and $|T|^2$ as functions of θ: (*a*) $\Omega/\Omega_0 = 0$, (*b*) 0.5, (*c*) 1.0, and (*d*) 1.5.

constant h, and perfect tuning, so that the wave amplitudes are independent of t. Waves are incident in the north-easterly direction so that $0 < \theta < \frac{1}{2}\pi$. The differential equations are

$$C_{g_1}\frac{\partial A}{\partial x}+C_{g_2}\frac{\partial A}{\partial y} = -\mathrm{i}\Omega_0 \cos 2\theta B, \tag{3.1}$$

$$-C_{g_1}\frac{\partial B}{\partial x}+C_{g_2}\frac{\partial B}{\partial y} = -\mathrm{i}\Omega_0 \cos 2\theta A. \tag{3.2}$$

These are hyperbolic partial differential equations where x and y play the roles of space and time respectively. Let us introduce the abbreviations

$$\alpha = \frac{C_{g_1}}{C_{g_2}} = \cot\theta > 0 \tag{3.3}$$

and

$$\beta = \frac{\Omega_0 \cos 2\theta}{C_g \sin\theta}. \tag{3.4}$$

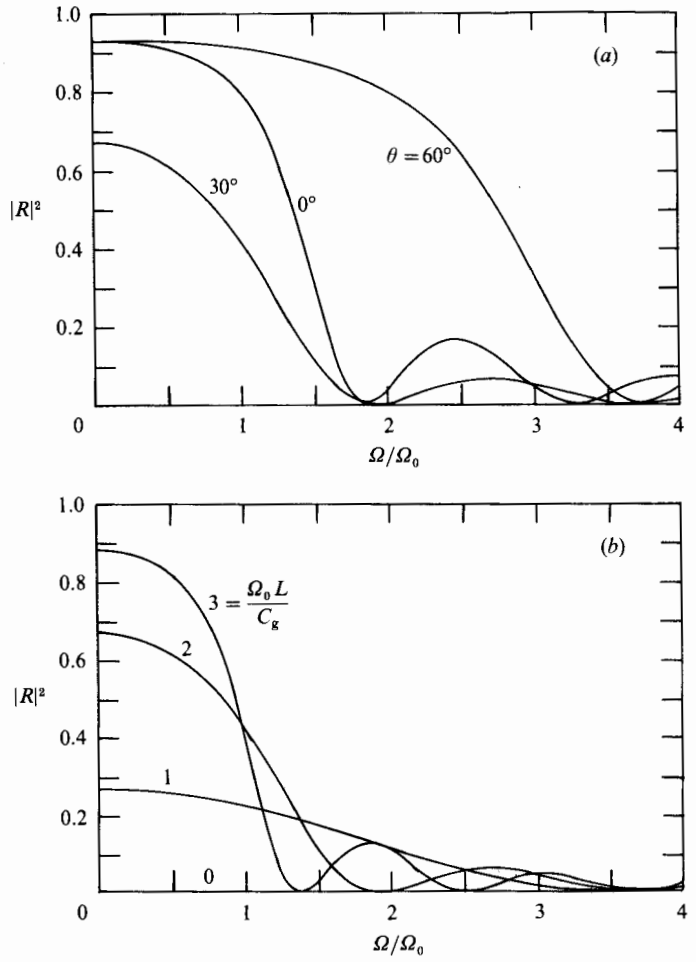

FIGURE 2. Reflection intensity as a function of detuning frequency: (*a*) $\Omega_0 L/C_g = 2$; (*b*) $\theta = 30°$.

Equations (3.1) and (3.2) may be rewritten as

$$\frac{\partial A}{\partial y} + \alpha \frac{\partial A}{\partial x} = -\mathrm{i}\beta B, \tag{3.5}$$

$$\frac{\partial B}{\partial y} - \alpha \frac{\partial B}{\partial x} = -\mathrm{i}\beta A, \tag{3.6}$$

which can be combined to give the Klein–Gordon equation

$$\frac{\partial^2 A}{\partial y^2} - \alpha^2 \frac{\partial^2 A}{\partial x^2} + \beta^2 A = 0. \tag{3.7}$$

Since there are two characteristics pointing into the bar region from the x-axis, two initial conditions are needed along $y = 0$. The y-axis being time-like, only one boundary condition along $x = 0$ is needed. The appropriate conditions are

$$A = A_0, \quad x = 0, \quad y > 0, \tag{3.8}$$

$$A = A_0, \quad x > 0, \quad y = 0, \tag{3.9}$$

$$B = 0, \quad x > 0, \quad y = 0. \tag{3.10}$$

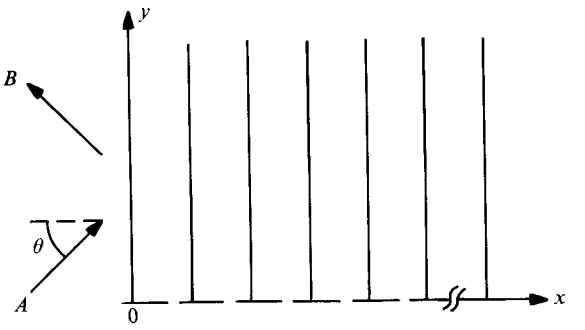

FIGURE 3. Two-dimensional scattering by the corner of a field of periodic bars. The bars are parallel to the y-axis and confined in the first quadrant.

Because of (3.9) and (3.10), (3.5) also implies

$$\frac{\partial A}{\partial y} = 0, \quad x > 0, \quad y = 0. \tag{3.11}$$

Equations (3.9) and (3.11) constitute the Cauchy data on the initial line $y = 0$.

By the usual technique of Fourier sine transform we get

$$\frac{A}{A_0} = \frac{2}{\pi}\int_0^\infty \mathrm{d}q \sin qx \left[\frac{q\alpha^2}{q^2\alpha^2+\beta^2} + \left(\frac{1}{q} - \frac{q\alpha^2}{q^2\alpha^2+\beta^2}\right)\cos(q^2\alpha^2+\beta^2)^{\frac{1}{2}}y\right]. \tag{3.12}$$

The first term can be easily inverted, giving

$$\frac{A(x,y)}{A_0} = \mathrm{e}^{-\beta x/\alpha} + \frac{2}{\pi}\beta^2\int_0^\infty \frac{\mathrm{d}q}{q}\sin qx \frac{\cos(q^2\alpha^2+\beta^2)^{\frac{1}{2}}y}{q^2\alpha^2+\beta^2}. \tag{3.13}$$

Let us denote

$$I = \alpha^2\int_0^\infty \frac{\mathrm{d}q}{q}\sin qx \frac{\cos(q^2\alpha^2+\beta^2)^{\frac{1}{2}}y}{q^2\alpha^2+\beta^2} \tag{3.14}$$

so that

$$A(x,y) = A_0\left[\mathrm{e}^{-\beta x/\alpha} + \frac{2}{\pi}\left(\frac{\beta}{\alpha}\right)^2 I\right]. \tag{3.15}$$

The following derivative can be evaluated explicitly:

$$\left.\begin{aligned} I_{xy} \equiv \frac{\partial I}{\partial x\,\partial y} &= -\int_0^\infty \mathrm{d}q \cos qx \frac{\sin(q^2\alpha^2+\beta^2)^{\frac{1}{2}}y}{(q^2\alpha^2+\beta^2)^{\frac{1}{2}}} \\ &= -\tfrac{1}{2}\pi\alpha J_0((\beta y)^2-(\beta y/\alpha)^2)^{\frac{1}{2}} \quad \text{if} \quad \alpha y > x > 0, \\ &= 0, \qquad\qquad\qquad\qquad\quad \text{if } \alpha y < x < \infty \end{aligned}\right\} \tag{3.16}$$

or

(Erdelyi 1953, p. 26, No. 30). Upon integration, we have for any x and y

$$I = \int_0^x \mathrm{d}x' \int_0^y \mathrm{d}y' I_{x'y'} + \frac{\pi}{2}\left(\frac{\alpha}{\beta}\right)^2 (1-\mathrm{e}^{-\beta x/\alpha}) \tag{3.17}$$

so that

$$\frac{A(x,y)}{A_0} = 1 + \frac{2}{\pi}\left(\frac{\beta}{\alpha}\right)^2 \int_0^x \mathrm{d}x' \int_0^y \mathrm{d}y' I_{x'y'}. \tag{3.18}$$

In (3.17) the integration constants have been chosen so that (3.8) and (3.9) are satisfied.

Let us introduce

$$X = \frac{\beta x}{\alpha} = \frac{\Omega_0 x}{C_g}\frac{\cos 2\theta}{\cos\theta}, \quad Y = \beta y = \frac{\Omega_0 y}{C_g}\frac{\sin 2\theta}{\sin\theta}. \tag{3.19}$$

In view of (3.16), we get from (3.18)

$$\frac{A(X, Y)}{A_0} = 1 - \int_0^Y \mathrm{d}X' \int_{X'}^Y \mathrm{d}Y' J_0((Y'^2 - X'^2)^{\frac{1}{2}}) \quad \text{if} \quad Y < X < \infty, \tag{3.20a}$$

$$\frac{A(X, Y)}{A_0} = 1 - \int_0^X \mathrm{d}X' \int_{X'}^Y \mathrm{d}Y' J_0((Y'^2 - X'^2)^{\frac{1}{2}}) \quad \text{if} \quad 0 < X < Y. \tag{3.20b}$$

In terms of X and Y, (3.5) becomes

$$\frac{\mathrm{i}B}{A_0} = -\frac{1}{A_0}\left(\frac{\partial A}{\partial X} + \frac{\partial A}{\partial Y}\right). \tag{3.21}$$

Carrying out the differentiation, we get

$$\frac{\mathrm{i}B(X, Y)}{A_0} = \int_0^Y \mathrm{d}X' J_0((Y^2 - X'^2)^{\frac{1}{2}}) \quad \text{if} \quad Y < X < \infty, \tag{3.22a}$$

$$\frac{\mathrm{i}B(X, Y)}{A_0} = \int_0^X \mathrm{d}X' J_0((Y^2 - X'^2)^{\frac{1}{2}}) + \int_X^Y \mathrm{d}Y' J_0((Y'^2 - X^2)^{\frac{1}{2}}) \quad \text{if} \quad 0 < X < Y. \tag{3.22b}$$

Note that both A and B are continuous across the characteristic line $Y = X$, i.e. $y = x\tan\theta$. In the region $Y < X$, A and B depend only on Y, implying that the presence of the boundary along $X = 0$ has no effect. For $Y > X$, A and B vary in both X and Y. Their variations are calculated by numerical integration and shown in figures 4 and 5. The reflection coefficient is simply

$$R = \frac{\mathrm{i}B(0, Y)}{A_0} = \int_0^Y \mathrm{d}Y' J_0(Y'). \tag{3.23}$$

Far from the ends of bars, $Y \gg 1$, reflection is complete.

We remark that there is, in principle additional local diffraction near the edge $Y = 0, X \geqslant 0$ and the first reflected ray $Y = -X$; this is neglected by the present geometrical optics approximation. However, B vanishes along, and is continuous across, both lines; only its normal derivative is discontinuous there. Thus this local diffraction is of minor significance. If desired, however, a correction can be constructed analytically by applying the parabolic approximation along these lines.

4. Bars on a sloping bed

In this section we examine the effects of bottom slope on the scattering by parallel bars. From our knowledge of the constant-depth case, the cutoff wavenumber, i.e. Ω_0/C_g must now vary with depth. If a wavetrain enters a strip of bars at a subcritical wavenumber $k+K$ with $K < \Omega_0/C_g$, it may cross the cutoff wavenumber somewhere over the bars, then become supercritical before leaving the strip. This and other features are now examined here for a seabed with a constant mean slope. For simplicity we further assume normal incidence from the left and constant bar amplitude D.

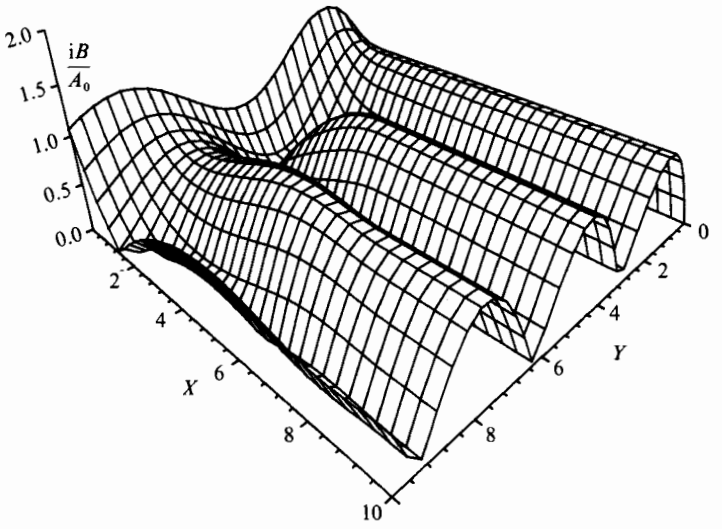

FIGURE 4. Variations of the reflected wave amplitude with X and Y, which are defined in (3.19).

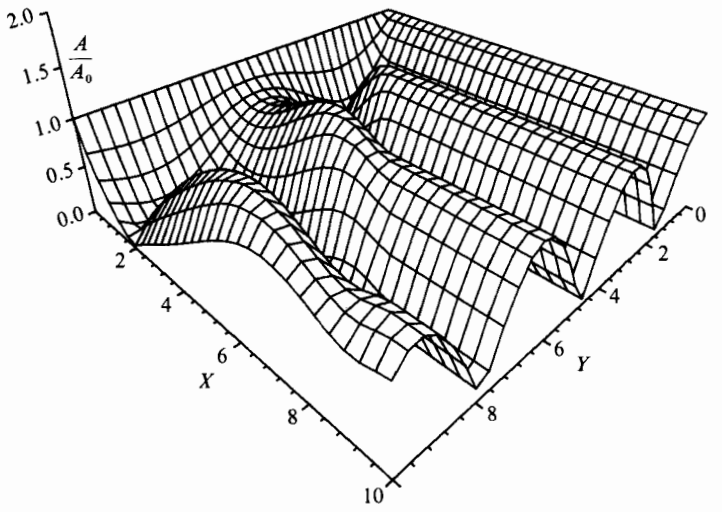

FIGURE 5. Variations of the transmitted wave amplitude with X and Y.

As sketched in figure 6, the origin $x = 0$ is chosen to coincide with the shoreward edge of the bar strip which has the width L. In this section the subscript zero denotes quantities evaluated at $x = 0$. The shoreline is along $x = L_1$, where all incident waves are absorbed by breaking. The bottom slope is h_0/L_1.

The governing equations are obtained from (1.1) and (1.2) by taking $\theta = 0$. Outside the strip of bars, the right-hand sides of these equations are zero. The boundary conditions at the edges of the bar strip are

$$[A]_{-L+0} = [A]_{-L-0}, \quad [B]_{-L+0} = [B]_{-L-0}, \tag{4.1}$$

$$[A]_{+0} = [A]_{-0} \quad [B]_{+0} = [B]_{-0}. \tag{4.2}$$

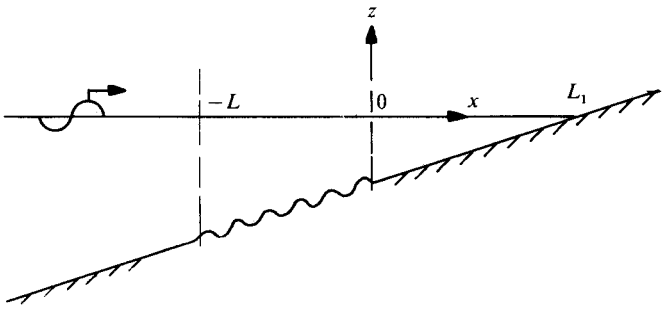

FIGURE 6. Bars on a sloping beach.

We now introduce the detuning time factor for A and B and the following transformation:

$$A C_g^{\frac{1}{2}} = \hat{A}\, e^{-i\Omega t}, \quad B C_g^{\frac{1}{2}} = \hat{B}\, e^{-i\Omega t}. \tag{4.3}$$

Equations (1.1) and (1.2) then become

$$-i\Omega\hat{A} + C_g \frac{d\hat{A}}{dx} = -i\Omega_0 \hat{B}, \tag{4.4}$$

$$-i\Omega\hat{B} - C_g \frac{d\hat{B}}{dx} = -i\Omega_0 \hat{A}. \tag{4.5}$$

Normalizing x by L and combining the two preceding equations, we then have

$$\frac{d}{dx}\left[\left(\frac{\Omega_0 L}{C_g}\right)^{-1}\frac{d\hat{B}}{dx}\right] + \left\{\frac{\Omega_0 L}{C_g}\left[\left(\frac{\Omega}{\Omega_0}\right)^2 - 1\right] + i\frac{d}{dx}\left(\frac{\Omega}{\Omega_0}\right)\right\}\hat{B} = 0. \tag{4.6}$$

Since complete breaking along the shoreline is assumed we have from (4.2) that

$$\hat{B} = 0 \quad \text{at} \quad x = 0. \tag{4.7}$$

Making use of (4.5) and (4.1) we also have

$$\frac{d\hat{B}}{dx} + i\frac{\Omega_0 L}{C_g}\frac{\Omega}{\Omega_0}\hat{B} = i\frac{\Omega_0 L}{C_g}\hat{A} \quad \text{at} \quad x = -1, \tag{4.8}$$

where the right-hand side is calculated from the conventional geometrical optics approximation of shoaling waves over a smooth bottom.

Equation (4.6) is of the Sturm–Liouville form

$$-\frac{d}{dx}\left[p(x)\frac{d\hat{B}}{dx}\right] + q(x)\hat{B} = 0, \quad -1 < x < 0, \tag{4.9}$$

with the boundary conditions

$$\hat{B} = 0, \quad x = 0, \tag{4.10}$$

$$\frac{d\hat{B}}{dx} + r\hat{B} = b, \quad x = -1. \tag{4.11}$$

Here

$$p(x) = -\left(\frac{\Omega_0 L}{C_g}\right)^{-1}, \quad q(x) = \frac{\Omega_0 L}{C_g}\left[\left(\frac{\Omega}{\Omega_0}\right)^2 - 1\right] + i\frac{d}{dx}\frac{\Omega}{\Omega_0}, \tag{4.12a, b}$$

$$r = i\left[\frac{\Omega_0 L}{C_g}\frac{\Omega}{\Omega_0}\right]_{-1}, \quad b = i\left[\frac{\Omega_0 L}{C_g}\hat{A}\right]_{-1}. \tag{4.12c, d}$$

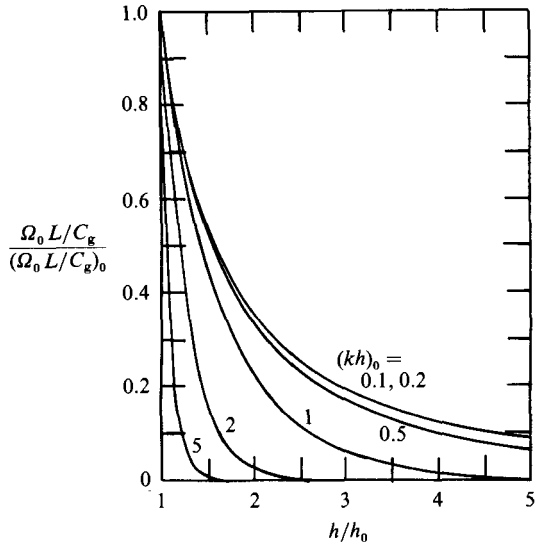

FIGURE 7. Local $\Omega_0 L/C_g$ normalized by its value at $x = 0$ *vs.* local depth for various incident wavenumbers.

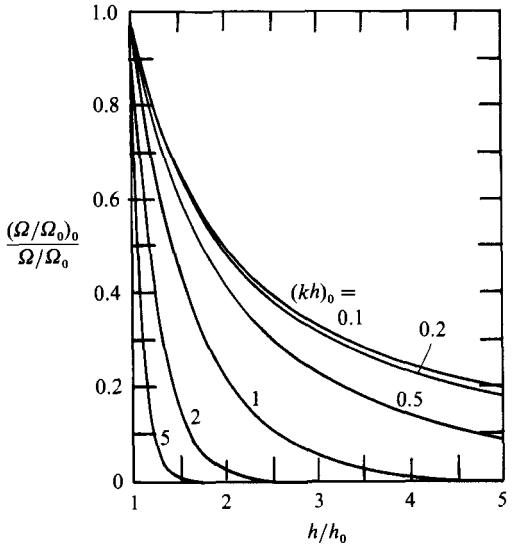

FIGURE 8. Local detuning frequency Ω/Ω_0 normalized by its value at $x = 0$ *vs.* local depth for various incident wavenumbers.

We may replace the boundary-value problem defined by (4.9)–(4.11) by requiring that the quadratic functional

$$F(\hat{B}) = -\int_{-1}^{0} \left\{ p\left(\frac{\mathrm{d}\hat{B}}{\mathrm{d}x}\right)^2 + q\hat{B}^2 \right\} \mathrm{d}x + [rp\hat{B}^2 - 2b\hat{p}B]_{-1} \tag{4.13}$$

be stationary for small variations in $\hat{B}$ with (4.10) as the essential and (4.11) as the natural boundary conditions. The method of finite elements is then used to solve for $\hat{B}$ at discrete points in the region $-1 < x < 0$.

Using $x = 0$ as the reference station, the numerical solution depends on the

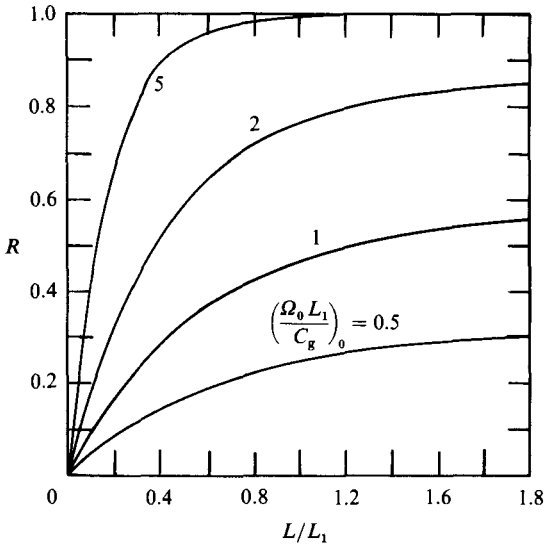

FIGURE 9. Reflection coefficient R *vs.* L/L_1.

dimensionless parameters kh, $\Omega_0 L/C_g$, Ω/Ω_0 and L/L_1. They represent respectively the local depth relative to the resonant wavelength, the width of the bar strip relative to the cutoff wavelength, the degree of detuning of the incident waves, and the location of the shoreline. In applications, we first may prescribe ω, Ω, h_0, D, L and L_1, then all these parameters can be inferred. In particular the bed slope is defined by h_0/L_1. The local values of $\Omega_0 L/C_g$ and $(\Omega/\Omega_0)^{-1}$ decrease rapidly with h/h_0 as shown in figures 7 and 8 where D is kept constant. For perfect tuning, the reflection coefficient at the incident edge of the strip ($R = |B/A|_{-1}$) is shown in figure 9 as a function of L/L_1 for several values of

$$\left(\frac{\Omega_0 L}{C_g}\right)_0 \frac{L_1}{L} = \left(\frac{\Omega_0 L_1}{C_g}\right)_0.$$

For fixed $(\Omega_0 L_1/C_g)_0$ reflection increases with L/L_1 but does not always approach unity. This is because as L/L_1 increases the left edge retreats to deeper water, while the transmission edge stays in the same depth. The bars furthest offshore then become too deep to be felt by the waves.

We now show the effect of detuning on the local amplitude of the incident and reflected waves. For a narrow strip (see figure 10*a*), the variation in x is monotonic, because the strip width is too small for spatial oscillations due to supercritical detuning to take effect. For a wide strip (see figure 10*b*), the oscillatory variation intensifies as $(\Omega/\Omega_0)_0$ increases. Local detuning becomes supercritical when Ω/Ω_0 exceeds unity. Take, for example, the case where $(\Omega/\Omega_0)_0 = 0.5$ and $(kh)_0 = 1$. This threshold occurs at the depth $h/h_0 = 1.45$, as can be seen from figure 8. This threshold is at $x = -0.45$ in figure 10*b*. Lastly, figure 11 shows the effect of detuning and strip width on the reflection at the left edge. As detuning or strip width increases the tendency for oscillation increases, as anticipated earlier.

The case of arbitrarily varying mean depth and oblique incidence can be examined in the same way.

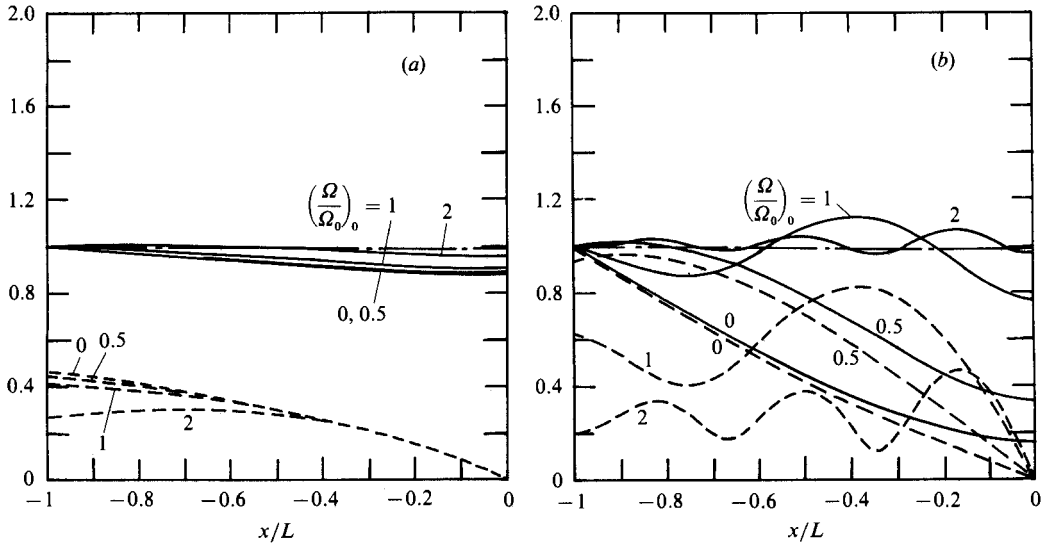

FIGURE 10. Transmitted and reflected wave amplitudes $|A/A_{-1}|$ (solid lines) and $|B/A_{-1}|$ (dashed lines) *vs.* x/L for D = constant, $(kh)_0 = 1$ and $L/L_1 = 1$. (*a*) $(\Omega_0 L/C_g)_0 = 1$, (*b*) $(\Omega_0 L/C_g)_0 = 5$. For comparison, $|A/A_{-1}|$ in the absence of bars is indicated by the dot–dash line.

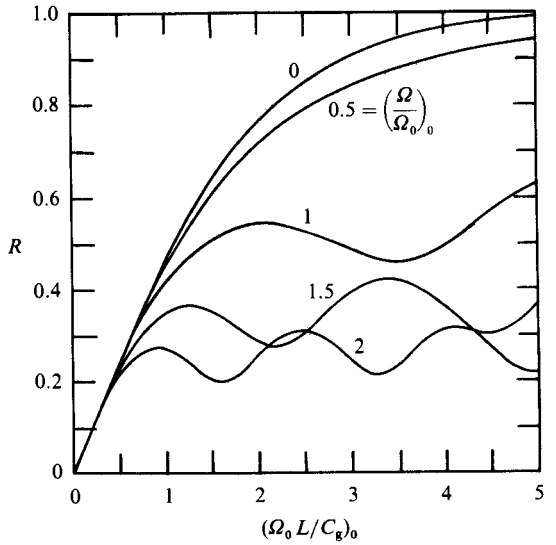

FIGURE 11. Reflection coefficient R *vs.* $(\Omega_0 L/C_g)_0$, for $(kh)_0 = 1$ and $L/L_1 = 1$.

5. Bars of other cross-sections

Neither natural sandbars are, nor man-made breakwaters likely to be, shaped as a sinusoidal curve. For economical construction breakwaters should be semicylinders of a simple cross-section such as a rectangle or a semicircle. It is therefore useful to assess the influence of the cross-sectional shape on the effectiveness of reflection. In general the profile of a seabed with bars should be a periodic function of x for many periods. Let the period be π/α and the incident wave be oblique and slightly detuned

from Bragg resonance, i.e. the wavenumber component in the x-direction is slightly different from α. We expand the bed profile as a Fourier series,

$$\delta(x) = \sum_{m=-\infty}^{\infty} \tfrac{1}{2} D_m \, \mathrm{e}^{2\mathrm{i}m\alpha x} \tag{5.1}$$

with $D_m = D_{-m}^*$. By following the analysis of Mei (1985) it is easily shown, for monochromatic waves, that only the first harmonic

$$\tfrac{1}{2}(D_1 \, \mathrm{e}^{2\mathrm{i}\alpha x} + D_{-1} \, \mathrm{e}^{-2\mathrm{i}\alpha x}) \tag{5.2}$$

will resonate reflected waves. Therefore it is only necessary to expand the shape function into a Fourier series and replace D in the previous analysis by D_1. Clearly if the incident wave has a finite spectral width, other harmonics in (5.1) may also contribute.

As two examples, we take a series of rectangular and half-elliptical cross-sections. The half-width is a and the height is b in each case:

$$\delta(x) = \begin{cases} b, & \text{if } \dfrac{|x|}{a} < 1 < \dfrac{\pi}{2\alpha a} \\ 0, & \text{if } 1 < \dfrac{|x|}{a} < \dfrac{\pi}{2\alpha a} \end{cases} \quad \text{(rectangles)}, \tag{5.3}$$

$$\delta(x) = \begin{cases} b\left[1 - \left(\dfrac{x}{a}\right)^2\right]^{\frac{1}{2}}, & \text{if } \dfrac{|x|}{a} < 1 < \dfrac{\pi}{2\alpha a} \\ 0, & \text{if } 1 < \dfrac{|x|}{a} < \dfrac{\pi}{2\alpha a} \end{cases} \quad \text{(half ellipses)}. \tag{5.4}$$

Mathematically speaking, these profiles have abrupt changes of slope and are not compatible with the perturbation theory. Therefore the results are valuable primarily as a guide for more accurate analysis. With this reservation, we give the Fourier coefficients

$$D_1 = \frac{2b}{\pi} \sin(2\alpha a) \quad \text{(rectangles)}, \tag{5.5}$$

$$D_1 = bJ_1(2\alpha a) \quad \text{(half ellipses)}. \tag{5.6}$$

For small αa, D_1 is approximately $(4/\pi)\alpha ab$ for the rectangle and αab for the ellipse. As αa increases, D_1 reaches a maximum and then decreases. When adjacent cylinders touch each other, a approaches $\pi/2\alpha$. At this limit D_1 vanishes for the rectangles; there is no more reflection since the bed becomes flat again. For touching ellipses $D_1 = 0.285b$; there is of course still some reflection since the bed is not flat.

We acknowledge the financial support of the Ocean Engineering Program, US Office of Naval Research and the Fluid Mechanics and Hydraulics Program, US National Science Foundation. Part of this study was initiated when C.C.M. was a guest at Norwave, Inc. Oslo, Norway. The warm and stimulating hospitality of Dr Even Mehlum and his colleagues there is recorded with pleasure.

REFERENCES

DAVIES, A. G. & HEATHERSHAW, A. D. 1984 Surface-wave propagation over sinusoidally varying topography. *J. Fluid Mech.* **144**, 419–443.

ERDELYI, A. 1954 *Tables of Integral Transforms.* MacGraw Hill.

HARA, T. & MEI, C. C. 1987 Bragg scattering of surface waves by periodic bars: theory and experiment. *J. Fluid Mech.* **178**, 59–76.

KIRBY, J. T. 1986*a* A general wave equation for waves over rippled beds. *J. Fluid Mech.* **162**, 171–186.

KIRBY, J. T. 1986*b* On the gradual reflection of weakly nonlinear Stokes waves in regions with varying topography. *J. Fluid Mech.* **162**, 187–209.

MCCABE, C. 1986 How Phillips is dealing with subsidence at Ekofisk. *Ocean Industry* February, 30–34.

MEI, C. C. 1985 Resonant reflection of surface water waves by periodic sandbars. *J. Fluid Mech.* **152**, 315–335.

YOON, S. B. & LIU, P. L. F. 1987 Resonant reflection of shallow-water waves due to corrugated boundaries. *J. Fluid Mech.* **180**, 451–469.